Appendix

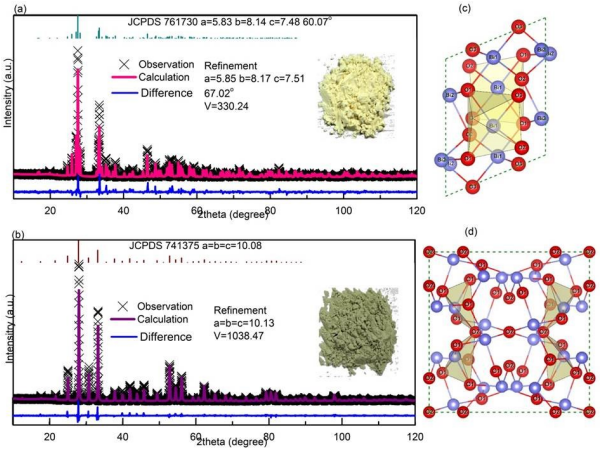

Figure S1 Rietveld refinement of α-Bi_2O_3 (a), and γ-Bi_2O_3 (b), as well as atomic structure model after structure relaxation (c) and (d)

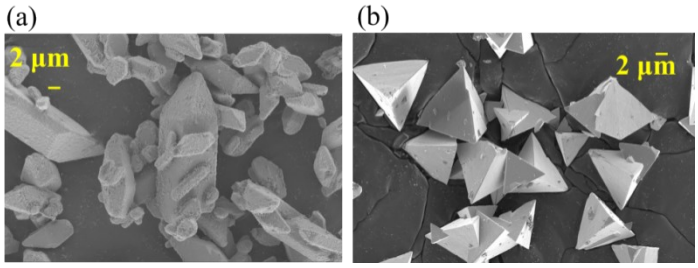

Figure S2 Morphology of (a) α-Bi_2O_3 and (b) γ-Bi_2O_3

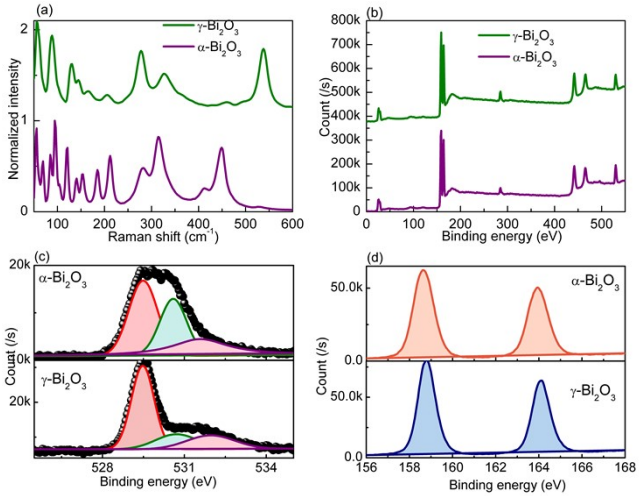

Figure S3 Raman spectrum (a), survey XPS and atomic percentage (b), high resolution O 1s (c), Bi 4f (d) spectra of other two phases

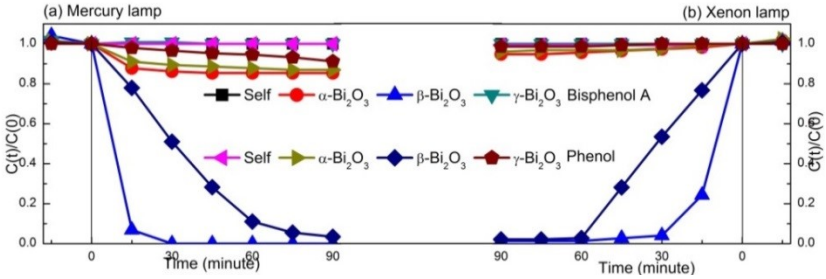

Figure S4 Degradation efficiency of bisphenol A and phenol upon irradiations of mercury lamp (a)

and xenon lamp (b)

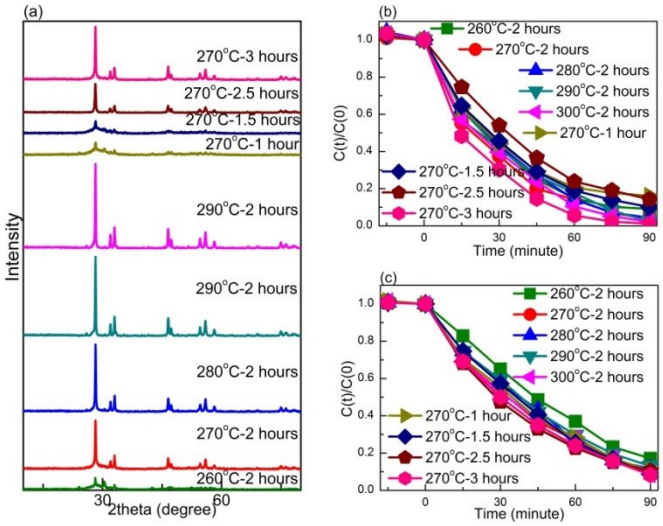

Figure S5 XRD of β-Bi_2O_3 calcined at different temperatures and durations (a), bisphenol A (b), and phenol (c) degradation efficiency curves

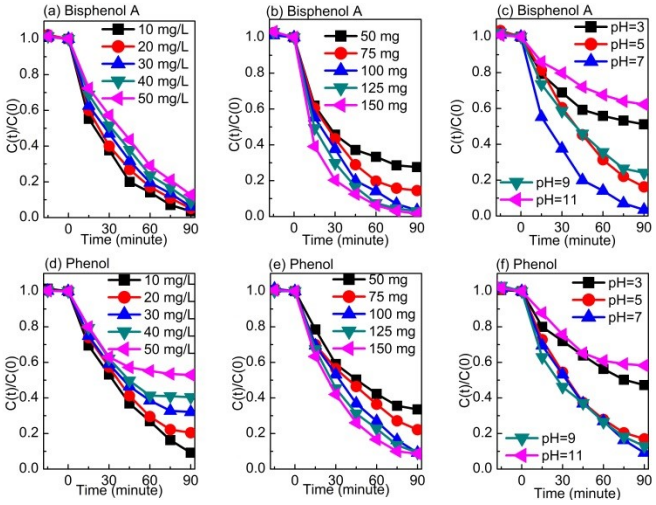

Figure S6 Bisphenol A (a-c) and phenol (d-f) degradation efficiency with different catalyzer mass, initial concentration, and pH

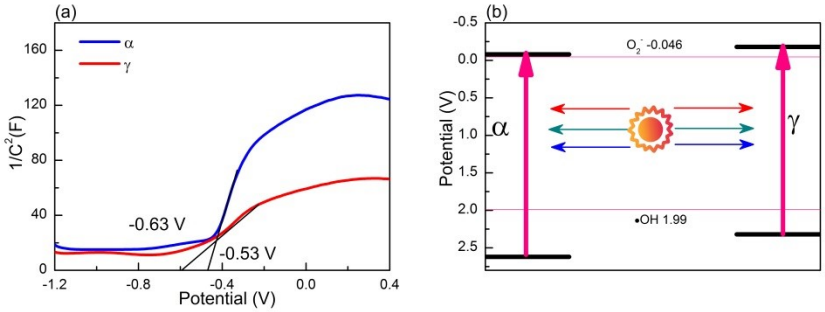

Figure S7 Mott-Schottky (a) and band edge potential (b) of the other two samples

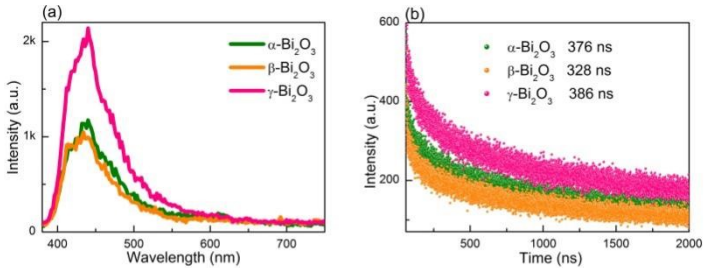

Figure S8 Photoluminescence spectra (a) and fluorescence lifetime (b) of three samples

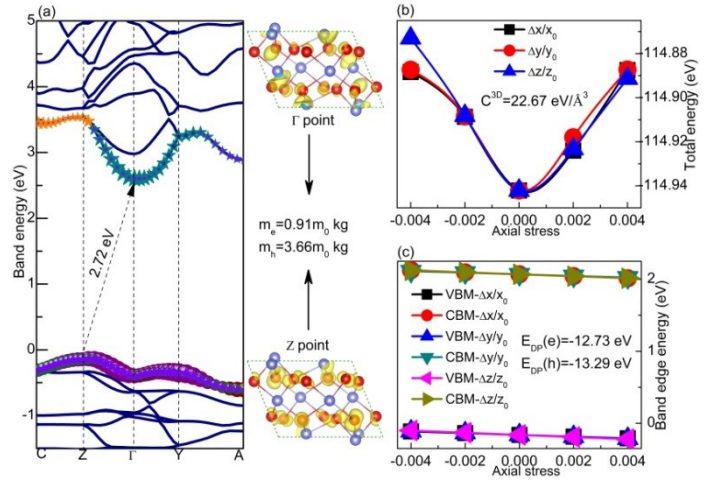

Figure S9 Energy band, VB top and CB bottom charge density with isovalue 0.005 e/Bohr^3 (a), total energy (b), VB top, and CB bottom position upon axial stress (c) in α-Bi_2O_3

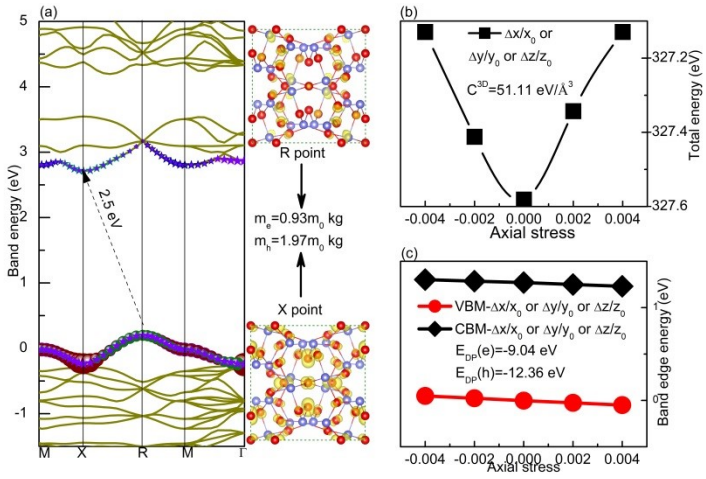

Figure S10 Energy band, VB top and CB bottom charge density with isovalue 0.005 e/Bohr^3 (a), total energy (b), VB top and CB bottom position upon axial stress (c) in γ-Bi_2O_3